Available online at www.sciencedirect.com

SCIENCE DIRECT®

Polymer Degradation and Stability 91 (2006) 2347–2356

Polymer Degradation and Stability

www.elsevier.com/locate/polydegstab

Thermal degradation kinetics and flame retardancy of phosphorus-containing dicyclopentadiene epoxy resins

Tsung-Han Ho [a], Tsu-Shang Leu [b,*], Yih-Min Sun [c], Jeng-Yueh Shieh [c]

[a] Department of Chemical Engineering, National Kaohsiung University of Applied Sciences, Kaohsiung 807, Taiwan, ROC
[b] Department of Chemical Engineering, Yung-Ta Institute of Technology and Commerce, Linlo, no. 316, Pingtung 909, Taiwan, ROC
[c] Department of Industrial Safety and Hygiene, Chung Hwa College of Medical Technology, Tainan 717, Taiwan, ROC

Received 12 February 2006; received in revised form 2 April 2006; accepted 4 April 2006

Abstract

The 2,6-dimethylphenol-dicyclopentadiene epoxy resin (MDE) was obtained by epoxidation of the intermediate 2,6-dimethylphenol-dicyclopentadiene novolac (MDN) which was synthesized from the reaction between dicyclopentadiene (DCPD) and 2,6-dimethylphenol. Subsequently, the 2,6-dimethylphenol-dicyclopentadiene advanced epoxy resin (MDAE) were prepared by reactions of 2-(6-oxido-6-H-dibenzo[c,e][1,2]oxaphosphorin-6-yl)-1,4-benzenediol (ODOPB) with MDE. The structure of MDN, MDE and ODOPB was confirmed by ^{1}H NMR, Fourier transform infrared (FTIR), elemental analyses (EA), mass spectroscopy (MS) and epoxy equivalent weight titration. Curing and thermal degradation kinetics of MDAE cured with diaminodiphenyl sulfone (DDS) were studied by the dynamic differential scanning calorimetry (DSC) and thermal gravimetric analysis (TGA), respectively. The activation energies of dynamic curing and thermal degradation were calculated by using the Kissinger and Ozawa's methods, respectively. The dynamic model gives a good description of curing kinetics up to a much wider temperature range. The relations concerning the activation energy of curing and phosphorous content of epoxy resins were discussed. The char yields and thermal stabilities of cured ODOPB-modified epoxy networks uniquely increase with ODOPB contents. The degradation temperatures (T_d, 5%) in nitrogen at a heating rate of 20 °C/min ranged from 344 to 401 °C, and the char yields at 800 °C are 11–24%. The activation energies of degradation ranged from 190 to 268 kJ/mol. High LOI value (found 33.8) could be achieved with a low phosphorus content around 1.0%, which implied that the flame retardancy was improved by the incorporation of ODOPB.

Keywords: Dicyclopentadiene phosphorus-containing epoxy resin; Thermal degradation kinetics; Flame retardant; TGA

1. Introduction

Epoxy resins were used widely in the polymer industry for surface coatings, adhesives, painting materials, pottings, composites, laminates, encapsulants for semiconductors, and insulating materials for electric devices, etc. [1–10], because they have excellent fluidity, chemical resistance, low shrinkage on cure, superior electrical and mechanical properties, and good adhesion to many substrates. Several approaches for modification of the epoxy backbone to enhance the thermal properties of epoxy resins have been reported [11–13]. However, the thermal stability and flammability of common epoxy system are the major disadvantages in their applications. The epoxy resin in use is mainly the diglycidyl ether of bisphenol A (DGEBA) and the tetrabromobisphenol A (TBBA), however, the bromine-containing advanced epoxy resin release hydrogen bromide, dibenzo-*p*-dioxin and dibenzo-furan during combustion, which cause corrosion and toxicity. Organic phosphates do not cause any of these problems. Organophosphorus compounds have demonstrated better ability as flame retardants for polymeric materials by forming a carbonaceous char, which acts as a physical barrier to heat transfer from the flame to the polymer and diffusion of combustible gas and smoke than halogen-containing compounds [14–21]. Flame retardants, phosphorus–halogen

---

* Corresponding author. Tel.: +886 8 7233733 362; fax: +886 8 7239840.
E-mail address: tsleu@mail.ytit.edu.tw (T.-S. Leu).

0141-3910/$ - see front matter © 2006 Elsevier Ltd. All rights reserved.
doi:10.1016/j.polymdegradstab.2006.04.002

mixtures, ammonium phosphate, and organophosphorus compounds have been used to impart flame retardancy to epoxy resins. Flame-retardant epoxy resins can be obtained by chemically bonding flame-retardant groups onto epoxy resins, and the permanent attachment of a flame retardant frequently leads to high efficiency in flame retardancy [22–24].

Hydrocarbon-containing epoxy resins, which were derived from the novolac of phenol and hydrocarbon in the presence of a Lewis acid, followed by epoxidization of the resulting hydrocarbon novolacs to epoxy resins. Among these hydrocarbons, dicyclopentadiene (DCPD) and higher oligomers of cyclopentadiene are the most commonly used starting materials because of their availability (DCPD is a by-product of C_5 streams in oil refineries), reactivity, and low cost. The structure of the 2,6-dimethylphenol–DCPD was introduced into the backbone to improve thermal property of the epoxy resins. In our laboratory, a rigid phosphorus-containing reactive 2-(6-oxido-6-H-dibenzo[c,e][1,2] oxaphosphorin-6-yl)-1,4-benzenediol (ODOPB) is synthesized and then incorporated to a 2,6-dimethylphenol-dicyclopentadiene epoxy resin, which is expected to exhibit the required flame retardancy, less fumes, and higher thermal stability than the conventional flame-retardant epoxy systems containing tetrabromobisphenol A. Kinetic characterization of thermosetting resins is the fundamental for understanding structure/property/processing relationships for manufacturing and utilization of high performance polymers. In this article, the effects of phosphorus contents on the thermal curing and thermal degradation behaviors of phosphorus-containing DCPD epoxy resins were studied by differential scanning calorimetry (DSC) and thermal gravimetric analysis (TGA) using dynamic experiments, respectively.

2. Experimental

2.1. Materials

Dicyclopentadiene (DCPD), 2,6-dimethylphenol, *p*-benzoquinone (BQ), and epichlorohydrin (ECH) were purchased from Acros. 4,4′-Diaminodiphenyl sulfone (DDS) was purchased from Chriskev. 9,10-Dihydro-oxa-10–phosphaphenanthrene 10-oxide (DOPO) from TCI and potassium hydroxide from Showa Co. were used as received. Ph_3P was triphenylphosphine, which was used as a curing accelerator. All solvents were commercial products (LC grade) and used without further purification.

2.2. Synthesis of 2,6-dimethylphenol–DCPD novolac (MDN) and its epoxy resin (MDE)

To a four-neck round-bottomed flask, equipped with a nitrogen inlet, stirrer, heating mantle, thermocouple, and temperature controller were added 2,6-dimethylphenol (1.42 mol) and $AlCl_3$ (0.03 mol). The reaction mixture was gradually heated to 120 °C, 0.2 mol of DCPD was added gradually over a period of 2 h, and the mixture was maintained at 120 °C for another 4 h. After the reaction was completed, 0.12 mol of 5 wt% aqueous sodium hydroxide was added, and the mixture was stirred for 1 h. The reaction mixture was filtered, and the filtrate was washed four times with deionized water. Next, the organic phase was separated and distilled in a rotary evaporator to remove excess 2,6-dimethylphenol. The crude products were dissolved in toluene and extracted with water for several times. The organic phase was distilled to remove toluene and water, and a deep-brown 2,6-dimethylphenol–DCPD novolac (MDN) was obtained in almost quantitative yield. The reaction scheme is shown in Scheme 1. MS (EI) *m*/*z* 376 (M+, 30); Elemental analyses for $C_{26}H_{32}O_2$: C = 82.90%, H = 8.60% (theoretically) and C = 82.59%, H = 8.63% (experimentally).

To a 1-L four-neck round-bottomed flask, equipped with a stirrer, heating mantle, thermocouple, temperature controller, and a Dean–Stark trap with a reflux condenser, were added 0.5 mol of the above synthesized MDN, 5 mol of ECH, and 80 g of the methyl ether of propylene glycol (1-methoxy-2-hydroxy propane) as a solvent. After stirring at room temperature and atmospheric pressure to thoroughly mix the contents, the temperature was raised to 65 °C and the pressure was reduced to 160 mm Hg absolute pressure. To the resultant solution was continuously added 42 g of a 40 wt% sodium hydroxide solution at a constant rate via a metering pump over a period of 3 h while maintaining the reaction temperature at 65 °C under a reduced pressure. During the addition of the NaOH solution, water was removed from the system by co-distilling with ECH and solvent; in the meantime distilled ECH and solvent were returned to the system. Upon completion of the addition, the reaction mixture was maintained at 65 °C for an additional 30 min. The resulting mixture was neutralized with a dilute aqueous potassium hydroxide solution and washed with deionized water. The organic phase was rotary evaporated at 180 °C under full vacuum over 3 h to remove the excess ECH and solvent. The residue was extracted with methyl isobutyl ketone (MIBK); the extract was washed four times with deionized water. The organic phase was separated and distilled to remove the solvents. A brown 2,6-dimethylphenol–DCPD epoxy resin (MDE) was obtained in almost quantitative yield (based on novolac). The reaction scheme is shown in Scheme 1.

2.3. Synthesis of ODOPB

To a 1-L four-neck round-bottomed reaction vessel equipped with a temperature controller, an overhead stirrer, and a reflux condenser were charged 500 g of ethoxyethanol and 270 g (1.25 mol) of DOPO; then, 122 g (1.13 mol) of powdered *p*-benzoquinone (BQ) was added incrementally. The temperature of the reaction mixture was raised to 125 °C, and the mixture was allowed to react at that temperature for 4 h. The resulted product was filtered and further recrystallized from ethoxyethanol to produce white solids. The yield of ODOPB is 97%, melting point of 254–256 °C (in Scheme 2). IR (KBr): 947 cm^{-1} (P–O–Ph), 1218 cm^{-1} (P=O), 3400 cm^{-1} (Ph–OH), 1580 cm^{-1} (P–Ph). MS (EI) *m*/*z* 324 (M+, 85); Elemental analyses for $C_{18}H_{13}O_4P$: C = 66.67%, H = 4.01%,

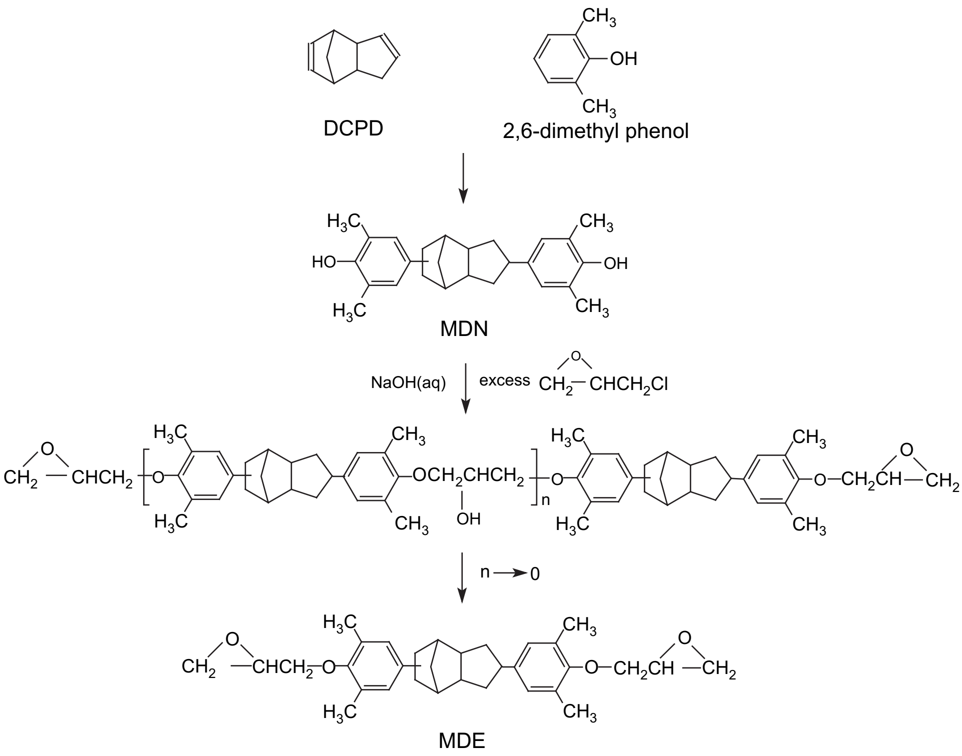

Scheme 1. The reaction scheme of MDN and MDE.

O = 19.74%, P = 9.52% (theoretically) and C = 66.54%, H = 4.05%, O = 20.04%, P = 9.29% (experimentally).

2.4. 2,6-Dimethylphenol-dicyclopentadiene advanced epoxy resin (MDAE) and their curing thermoset

To determine MDAE with sufficient content of phosphorous (i.e. 0.5, 1.0, 1.5 and 2.0 wt%) needed to achieve flame retardancy, various amounts of ODOPB were reacted with MDE at 160 °C for 90 min in the presence of 500 ppm ethyltriphenyl phosphonium acetate catalyst, as shown in Scheme 3. Subsequently, the advanced epoxy resins were mixed with an equal equivalent of curing agent (DDS) and 2×10^3 ppm Ph_3P in a mill at moderate temperature to give a thermosettable epoxy resin powder, which can be used for curing behavior study using a DSC. The resin powder was also cured in a hot press mould at temperature of 150 °C and 50 kg/cm^2 for a period of 1 h and then post-cured at 180 °C for 2 h and 210 °C for 3 h to obtain a cured sample.

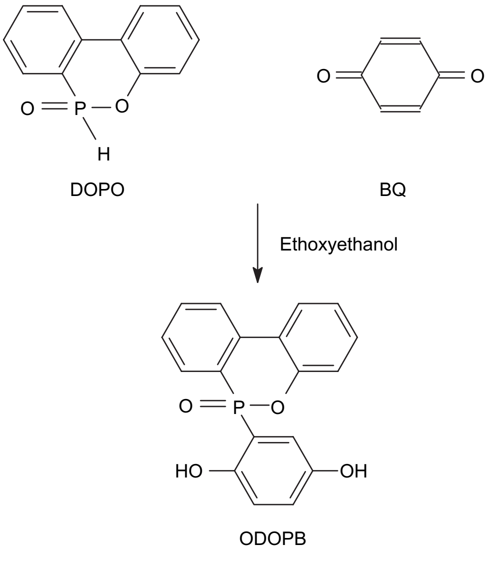

Scheme 2. The synthesis of monomer ODOPB.

2.5. Measurement and testing

^1H NMR spectra were registered using a Bruker AMX-400 and VARIAN INOVA-500 spectrometer using DMSO-d_6 as a solvent. Fourier transform infrared (FTIR) spectra were recorded on a Perkin–Elmer 16PC type spectrometer with KBr pellets, and the spectra were obtained in the optical range of 400–4000 cm^{-1}. EI (Electron Impact) source mass spectrometric analyses were performed on a VG 70-250S GC/MS spectrometer with a solid inlet. The epoxy equivalent weight (*EEW*) of the epoxy resin was determined by the $HClO_4$/potentiometric titration method in which the solution was used as a titrant, and the end points were detected by the first derivative of the potential versus the volume of the titrant. Differential scanning calorimeter (Perkin–Elmer DSC-7) measurements were used in this study. Samples of approximately 5–8 mg in weight were sealed in hermetic aluminum pans and scanned in the calorimeter with various heating rates of 5, 10, 20 and 30 °C /min in the range of 40–400 °C; under N_2 atmosphere and the peak temperature (T_p) was taken as the

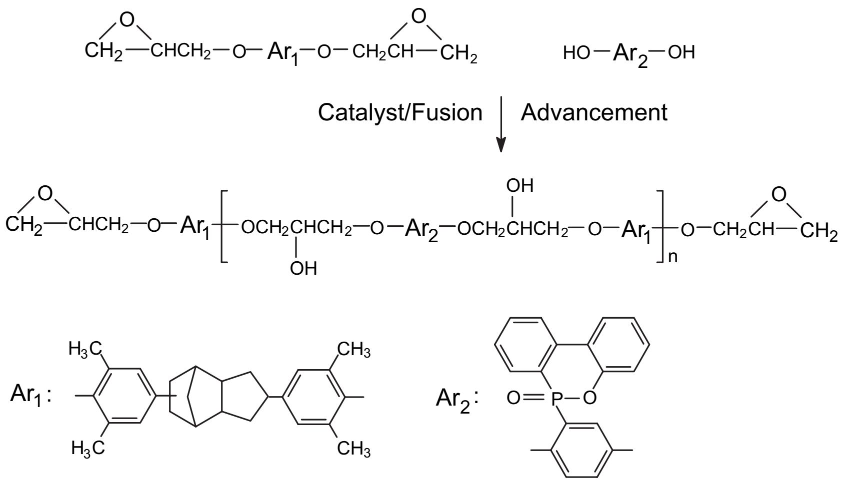

Scheme 3. The advancement of epoxy from MDE with ODOPB.

point of the reaction rate curve at the maximum peak temperature value between the onset temperature T_i and final temperature T_f, and peak baseline of reaction enthalpy ($-\Delta H$) was determined from the horizontal straight method. For dynamic scanning, calibration of the calorimeter was conducted for the heating rate using an indium standard. Thermal gravimetric analyses (TGA) were performed on a Perkin–Elmer TGA-7 thermal analyzer (7–10 mg samples) using various heating rates of 5, 10, 20 and 40 °C/min in N_2 at a purge pressure of 25 psi within the temperature range of 30–800 °C. The rapid weight loss temperature (T_r) was measured by taking first derivative from thermogravimetric analyzer curve. The LOI was determined with an Atlas Limiting Oxygen Index Chamber according to the standard procedure (ASTM D-2863-77). The percentage of O_2 in the O_2/N_2 mixture just sufficient to sustain the flame was taken as the LOI.

2.6. Sample codes

The sample codes for the various epoxy systems are designated MDE and MDAE, respectively. MDE stands for 2,6-dimethylphenol-dicyclopentadiene epoxy resin and MDAE stands for 2,6-dimethylphenol-dicyclopentadiene advanced epoxy resin. Because of various phosphorus contents of MDAE, the systems are designated MDAE*X*, and the number *X* after the MDAE is the weight percentage of the phosphorus. However, the cured epoxy systems are designated MDES and MDAE*X*S, S stands for curing agent of 4,4′-diaminodiphenyl sulfone (DDS). The various epoxy resins are MDES, MDAE0.5S, MDAE1.0S, MDAE1.5S and MDAE2.0S.

3. Results and discussion

3.1. Characterization of MDN and MDE

The IR spectra of MDN and MDE are shown in Fig. 1. The characteristic absorption peaks of −HC=CH− (from DCPD) at 770–690 and 3040–3010 cm^{-1} have disappeared as in Fig. 1A, implying that all −HC=CH− functional groups had reacted with 2,6-dimethylphenol. The characteristic absorption peaks of the aromatic ring at 1473 cm^{-1} and the OH absorption peaks of novolac at 3421 cm^{-1} are observed in Fig. 1A. The IR spectrum of MDE is shown in Fig. 1B, and shows similar absorption peaks with DCPD type novolac of IR spectrum at 1473 cm^{-1} of benzene and 2947 cm^{-1} of methyl. The OH absorption peak at 3421 cm^{-1} almost has disappeared, and another epoxy group absorption peak at 930 cm^{-1} appeared. Fig. 2 shows the ^1H NMR spectrum of MDN. The characteristic peaks for MDN of the aromatic Hs at 7.2–7.5 ppm, OH group at 7.8 ppm, and aliphatic Hs at

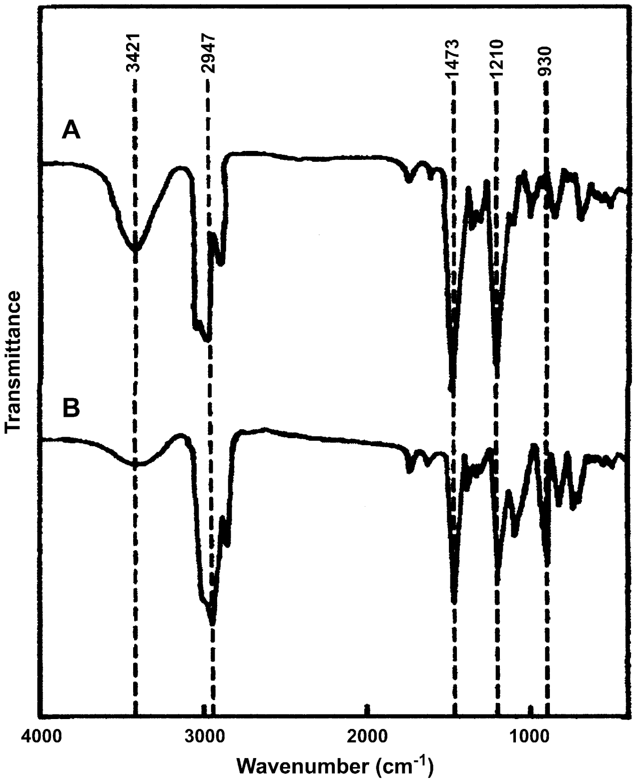

Fig. 1. FTIR spectra of (A) MDN and (B) MDE.

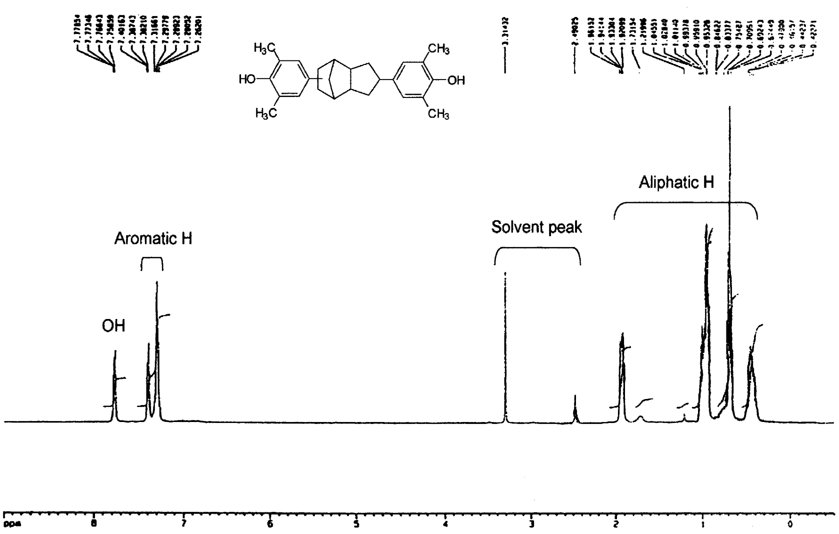

Fig. 2. ^{1}H NMR spectrum of MDN.

0.3–2.0 ppm are observed. The epoxy group is determined by back-titration with perchloric acid using Crystal Violet indicator [25]. The end point can be determined potentiometrically, and applications of the method have been reported to show good results [26–28]. The *EEW* value of synthesized 2,6-dimethylphenol–DCPD epoxy resin is 250 g/equiv, which is close to the theoretical *EEW* of 244 g/equiv, hence the typical product contained ca. 98% by weight of the MDE (i.e. minimize high molecular weight species, see Scheme 1) [29], where the *n* value is ca. 0.03 (approaches zero).

3.2. Characterization of ODOPB and advanced epoxy resin of MDAE

The ODOPB (including reactive, phosphorus-containing rigid and heterocyclic structure) was synthesized by the addition of DOPO to BQ in a quantitative yield. The reaction scheme is shown in Scheme 2. Fig. 3 shows the ^{1}H NMR spectrum of ODOPB. The characteristic peaks for ODOPB of the aromatic Hs at 6.61–8.22 ppm and OH group at 9.18–9.42 ppm are observed. The ratio of integration area of phenolic Hs/aromatic Hs is 1.99:11.12 = 1:5.59, which agrees with the theoretical value of 2:11 = 1:5.50. As the reaction proceeded, the disappearance of distinctive absorption at 2275–2240 cm^{-1} for P–H stretching of DOPO was observed, whereas a broad phenolic OH vibration absorption peak around 3400 cm^{-1} appeared in ODOPB as shown in Fig. 4. For the aforementioned process (directly from MDN and excess ECH), preparation of the higher molecular weight species is subject to practical limitations. An alternative method is the chain extension reaction of short-chain epoxy (crude MDE) with ODOPB, this method is sometimes referred to as the advancement process. Epoxy resins with various phosphorus contents have been prepared by applying the advancement of 2,6-dimethylphenol–DCPD epoxy resin with ODOPB. The reaction scheme is shown in Scheme 3. Their epoxy equivalent

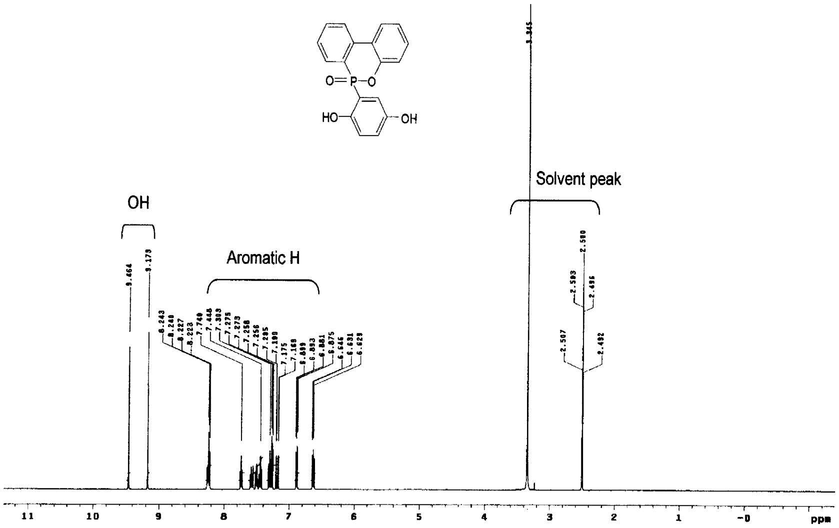

Fig. 3. ^{1}H NMR spectrum of ODOPB.

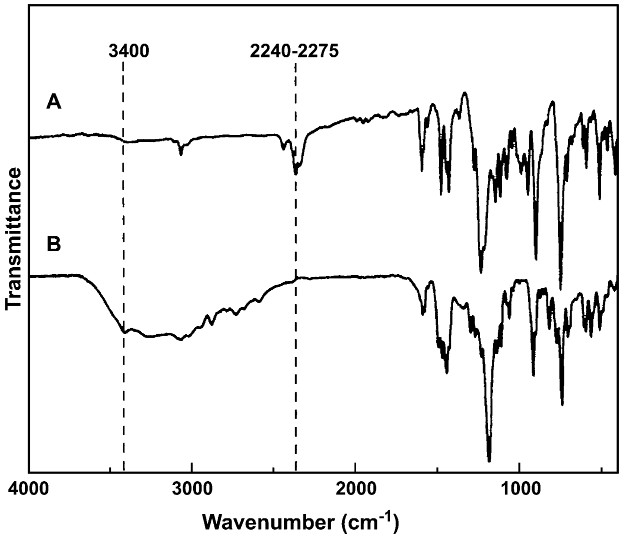

Fig. 4. FTIR spectra of (A) DOPO and (B) ODOPB.

weights (*EEWs*) are measured as shown in Table 1. The molecular structure of these advanced epoxy resin was rather similar, also, they had almost same patterns and IR spectra are shown in Fig. 5. The characteristic absorption peak at 1045 cm^{-1} is due to the P–O stretching vibration of phosphorus compounds, P=O stretching at 1246 cm^{-1}, P–phenol absorption peak at 1585 cm^{-1}, and an epoxy absorption peak at 929 cm $^{-1}$. Due to the advancement of epoxy resin, curing of epoxy resin has resulted in opening of epoxy ring to produce secondary hydroxyl group. The characteristic absorption peak of OH at 3400 cm^{-1} is evident in Fig. 4(B).

3.3. Curing behavior

DSC thermograms of various phosphorus contents of thermosettable epoxy resins at a heating rate of 10 °C/min (other DSC scans not shown) were shown in Fig. 6. The exothermic temperatures ranged around from 160 to 330 °C were observed. Generally, a curing system exhibiting a lower exothermic peak temperature under the same set of curing conditions is more reactive of the epoxy resins. The results show that all the exothermic peak of the ODOPB-modified epoxy resins have shifted to the higher temperature. Furthermore, the ODOPB with the bulky rigid ring structure, which interferes the molecular movement and slows down the curing process, as a fact of result, the reaction temperature increased.

Table 1
EEW of epoxy measured via potentiometry

Epoxy	P content (%)	*EEW* (g/equiv)	
		Found	Calcd.
MDES	0	250	244
MDAE0.5S	0.5	308	
MDAE1.0S	1.0	364	
MDAE1.5S	1.5	447	
MDAE2.0S	2.0	580	

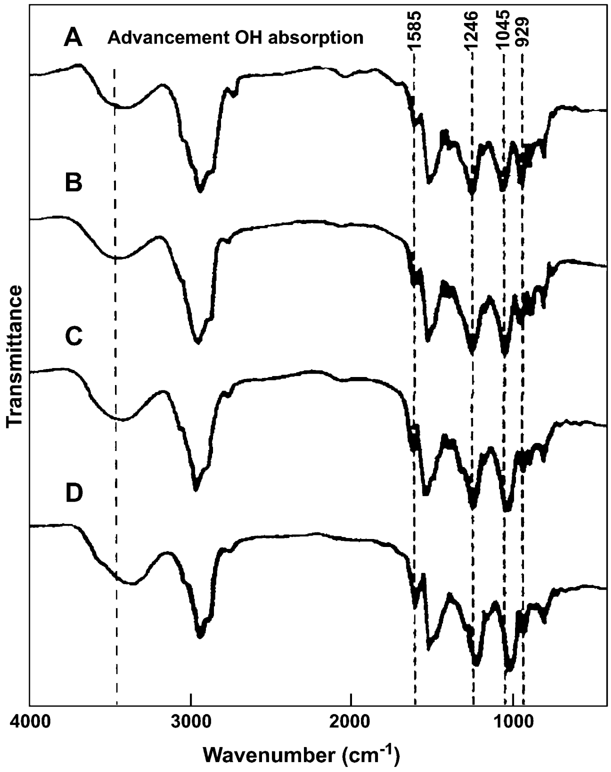

Fig. 5. FTIR spectra of advancement of epoxy (A) MDAE0.5S, (B) MDAE1.0S, (C) MDAE1.5S and (D) MDAE2.0S.

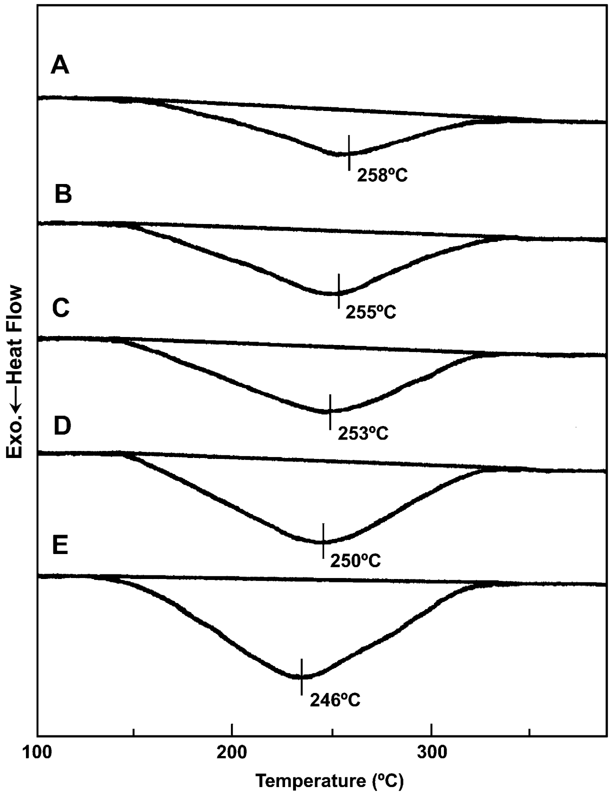

Fig. 6. DSC traces of the various epoxy resins at a constant heating rate of 10 °C/min (A) MDAE2.0S, (B) MDAE1.5S, (C) MDAE1.0S, (D) MDAE0.5S and (E) MDES.

This phenomenon can be explained by the measuring of activation energy of curing reaction as shown below.

DSC examined various phosphorus contents of thermosettable epoxy resins under the heating rate of 5, 10, 20 and 30 °C /min. The curing behaviors of dynamic DSC heating scans that increased the heating rate caused the curing exothermic curves to shift to the higher temperature. Table 2 shows the DSC data of various samples, which indicates the more phosphorus content, which means the more phosphorus-containing bulky rigid DOPO in the MDAE resins, the lower exothermic heat of reaction ($-\Delta H$), this might be explained by the *EEW* increased or in another word the reactive epoxy ring is reduced.

3.4. Kinetic of thermal curing by DSC

The general mathematical model to describe the kinetics of a system undergoing chemical change is

$$r = \frac{dx}{dt} = k(T)f(x) \tag{1}$$

where r is the rate of reaction, x is the degree of polymerization or degradation. From Eq. (1), it can be seen that the rate is both a function of temperature, given by $k(T)$, and a function of the degree of conversion, given by $f(x)$. The rate of reaction corresponds to the height (with respect to the base line) of the DSC curve at a given temperature, $k(T) = k_0 \exp(-E/RT)$ is the apparent rate constant, k_0 the pre-exponential factor, and E the apparent activation energy. For a multiple bond polymerization, nth-order kinetics has always been reported, hence, for dynamic system, Eq. (1) can be rewritten as

$$r = \Phi\frac{dx}{dT} = k_0 e^{-E/RT}(1-x)^n \tag{2}$$

where Φ is the heating rate (i.e. $\Phi = dT/dt$), the apparent activation energy of the curing reaction can be obtained by dynamic DSC scans. The data from two dynamic methods are analyzed by the following methods.

Table 2
Thermal behaviors at different heating rates of polymers

Sample code	Φ (°C/min)	T_i[a] (°C)	T_p[b] (°C)	T_f[c] (°C)	$-\Delta H_{ave}$[d] (J/g)
MDES	5	150	232	310	146.0
	10	153	246	329	
	20	160	275	333	
	30	178	290	342	
MDAE0.5S	5	154	234	314	136.8
	10	158	250	332	
	20	163	275	343	
	30	173	292	360	
MDAE1.0S	5	156	237	328	123.5
	10	157	253	336	
	20	165	277	352	
	30	175	294	366	
MDAE1.5S	5	155	239	330	96.1
	10	151	255	337	
	20	171	275	353	
	30	184	295	368	
MDAE2.0S	5	161	240	332	49.5
	10	166	258	340	
	20	175	278	345	
	30	193	294	370	

[a] Temperature at initial (onset) rate of reaction.
[b] Temperature at maximum (peak) rate of reaction.
[c] Temperature at final rate of reaction.
[d] Heat of polymerization (average values).

3.4.1. Kissinger's method [30]

The reaction rate curves at the peak maximum temperature (T_p) is defined by

$$\left[\frac{d}{dT}\left(\frac{dx}{dt}\right)\right]_{T_p} = 0 \tag{3}$$

From Eq. (3), it was observed that the extent of reaction at the peak temperature (T_p) is a constant (i.e. specific maximum value) and independent of the heating rate for many thermosetting systems. By differentiation and taking its logarithmic form, we obtain

$$-\ln\left(\frac{\Phi}{T_p^2}\right) = \ln\left[\frac{E/R}{k_0 n(1-x_p)^{n-1}}\right] + \frac{E}{RT_p} \tag{4}$$

where x_p is the peak conversion. The Eq. (4) yields linear plots of $-\ln(\Phi/T_p^2)$ against ($1/T_p$), the apparent activation energy that can be obtained from the slope of the corresponding straight line for all samples is given in Fig. 7, and these values are summarized in Table 3.

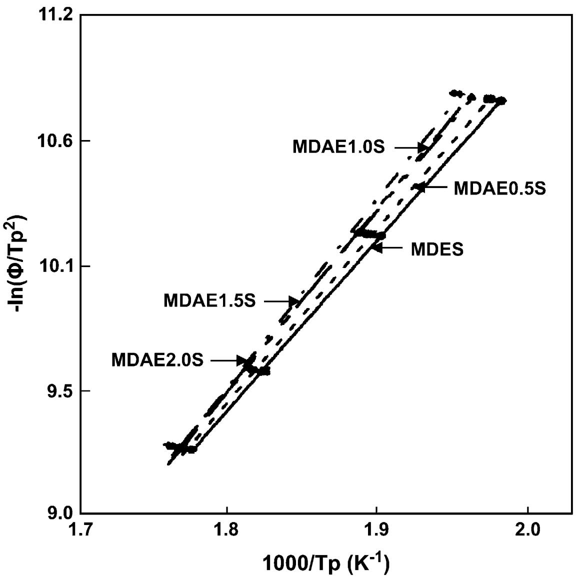

Fig. 7. Plots of $-\ln(\Phi/T_p^2)$ versus $1/T_p$ by using the Kissinger's method, the corresponding sample codes from right to left (MDES, MDAE0.5S, MDAE1.0S, MDAE1.5S and MDAE2.0S).

Table 3
The activation energies of polymerization obtained from the Kissinger's and Ozawa's methods

Epoxy	E (kJ/mol)	
	Kissinger	Ozawa
MDES	69.7	64.5
MDAE0.5S	71.1	65.9
MDAE1.0S	72.9	67.8
MDAE1.5S	74.5	69.5
MDAE2.0S	76.4	71.5

3.4.2. Ozawa's method [31,32]

Another theoretical treatment, namely, the Ozawa's method can also be applied to the thermal data. The resulting equation can be formulated as follows

$$\frac{1}{2.303}\ln \Phi = -0.4567\frac{E}{\mathrm{R}T} + \left[\log\frac{k_0 E}{\mathrm{R}} - \log F(x) - 2.315\right] \quad (5)$$

where $F(x)$ is the conversion dependent function, the method has been modified by Doyle [33] and is shown in the following

$$-\ln \Phi_1 - 1.052\frac{E}{\mathrm{R}T_1} = -\ln \Phi_2 - 1.052\frac{E}{\mathrm{R}T_2} = \cdots \quad (6)$$

The apparent activation energy for the curing of thermosetting resin can be obtained by plotting natural logarithm Φ against the reciprocal of the maximum temperature by using

$$E = -\frac{\mathrm{R}}{1.052}\left[\frac{\Delta \ln \Phi}{\Delta\left(1/T_{\mathrm{p}}\right)}\right] \quad (7)$$

If the resulting extent of reaction at the peak temperature (T_{p}) changes with the heating rate, it would not be proper to use Eq. (6). The apparent activation energy was calculated from Fig. 8 and Table 3. The resulting apparent activation energies using the two methods were quite close. The E tends to be higher with increasing the phosphorus content, it indicates that the curing temperature increases with the size of bridging group between two oxiranes. The fact is consistent with the exothermic heat of reaction ($-\Delta H$) observed by DSC.

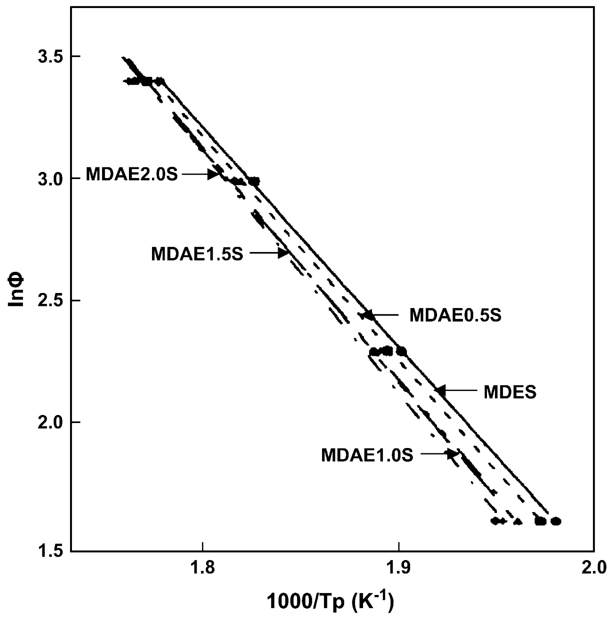

Fig. 8. Plots of ln Φ versus $1/T_{\mathrm{p}}$ by the Ozawa's method. The corresponding sample codes from right to left (MDES, MDAE0.5S, MDAE1.0S, MDAE1.5S and MDAE2.0S).

3.5. Thermal gravimetric analysis (TGA)

The thermal properties of each sample were analyzed by TGA, as shown in Table 4. The typical thermal weight loss curvatures are shown in Fig. 9. TGA traces of cured epoxy provided additional information regarding their thermal stability and thermal degradation behavior. The results of the TGA analyses showed an excellent thermal stability of the synthesized copolymers. The 5 wt% losses in N_2 atmosphere were at 339 °C and the char yields at 800 °C was 11% for MDES, and the corresponding values were in the range of 375–387 °C and 14–21% for MDAES (phosphorous content is from 0.5 to 2.0) system at a heating rate of 10 °C/min. The 5 wt% degradation temperature (T_{d}) and char yield of MDES systems were lower than those of corresponding MDAES systems. The results suggest a high thermal stability of the strong enthalpic interactions inherent in polymer backbone, and special advancement (i.e. ODOPB, involving bulky pendant chain and ring compound, P–O, P=O degradation energy is 340 and 544 kJ/mol, respectively) molecular structure. In addition, their char yields increased with the phosphorus content.

Fig. 10 showed the relationship between the content of flame retarding element and the LOI values, the LOI

Table 4
Thermal stability and flame retardant of polymers

Sample code	Φ (°C/min)	T_{d}[a] (5%) (°C)	T_{d} (10%) (°C)	T_{r}[b] (°C)	Char yield 800 °C (%)	LOI
MDES	5	328	344	369	10	26.7
	10	339	350	378	11	
	20	344	364	392	11	
	30	361	372	406	13	
MDAE0.5S	5	349	364	400	13	28.9
	10	375	388	409	14	
	20	390	401	422	14	
	30	396	403	435	16	
MDAE1.0S	5	372	395	408	16	33.8
	10	381	401	418	17	
	20	394	406	431	20	
	30	400	417	442	21	
MDAE1.5S	5	376	404	422	18	34.2
	10	382	405	437	19	
	20	399	407	447	23	
	30	405	425	455	24	
MDAE2.0S	5	383	415	436	20	35.0
	10	387	408	443	21	
	20	401	408	456	24	
	30	412	431	467	26	

[a] Temperature for decomposition of 5% weight loss.
[b] Temperature of maximum rate of weight loss.

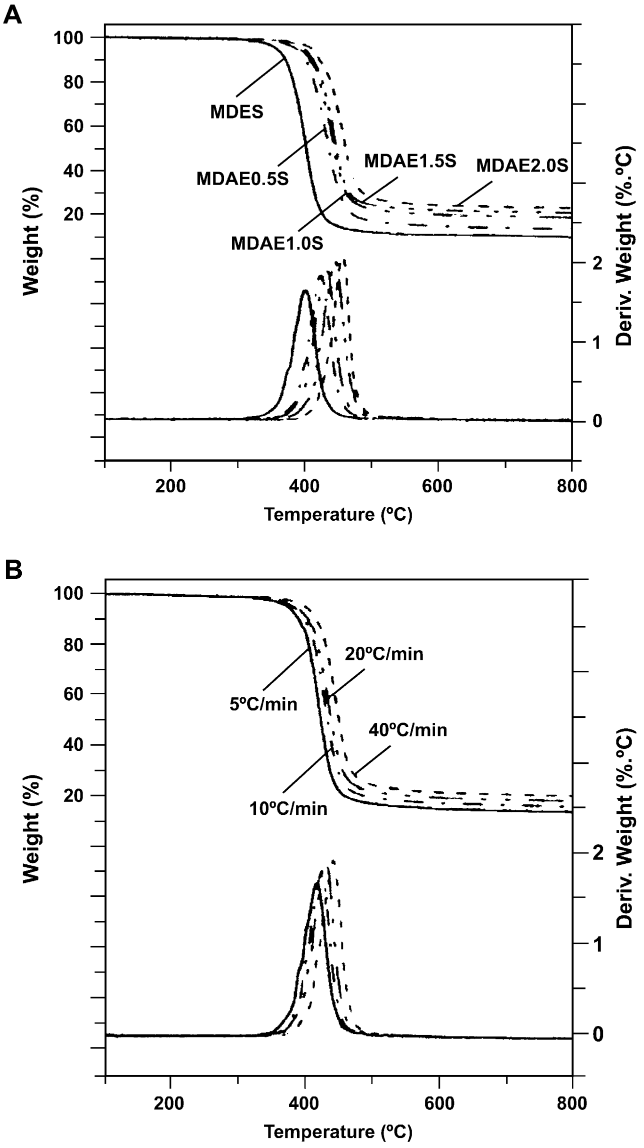

Fig. 9. TGA curves of (A) various epoxy resins at a constant heating rate of 20 °C /min (B) MDAE1.0S at different heating rates under nitrogen.

increased drastically from 26.7 to 33.8 when the phosphorus content added around 1.0%. However, it reached a plateau when the phosphorus content exceeded 1.0%. Adducts of ODOPB can be used for chain extension of epoxy resin and because of aromatic, phosphine oxide of resultant epoxies, a relatively low content of phosphorus is needed for high LOI values. Phosphine oxide structures are often used to impart flame retardancy, because they are thermally and hydrolytically very stable. Phosphorus-containing MDAES showed higher LOI than non-phosphorus-containing MDES. This also explains that phosphorus contained slag provides a covered film to interfere the combustion air to go in deeper and slows down the cracking of inner molecules, which decrease the combustion rate. Hence, epoxy with ODOPB caused these advanced epoxy resins to exhibit high thermal stability and better flame retardancy.

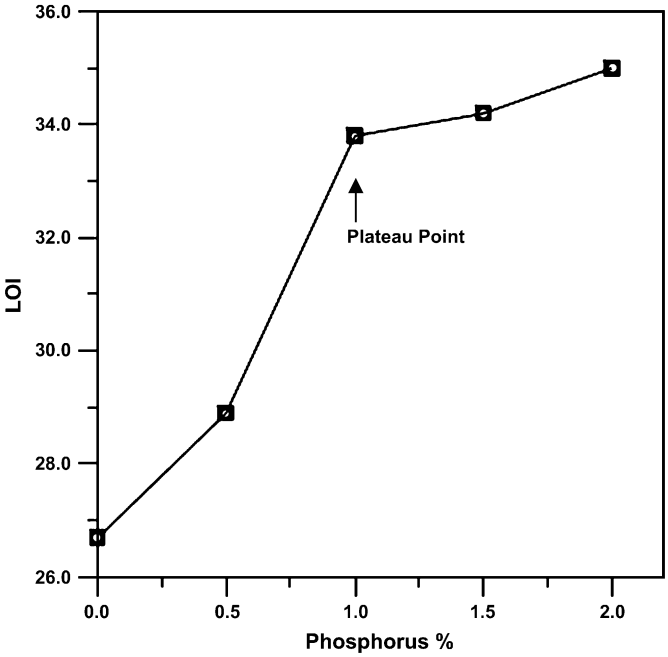

Fig. 10. LOI versus the phosphorus weight contents relation of various epoxy resins.

3.6. Thermal degradation kinetic behavior

Flynn and Wall [34] derived that the results of thermal degradation kinetics are consistent with Ozawa. The hardened epoxy resins were heated up at different heating rates and the relationship between degree of conversion and temperature can be expressed by Arrhenius equation. Therefore, the polymer thermal degradation is expressed as in formula (8)

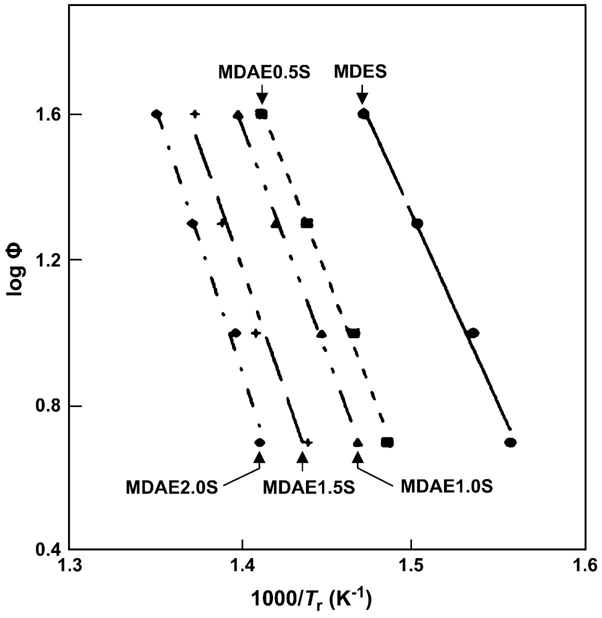

Fig. 11. The activation energies for the degradation reaction of various epoxy resins through Ozawa's method. The corresponding sample codes from right to left (MDES, MDAE0.5S, MDAE1.0S, MDAE1.5S and MDAE2.0S).

Table 5
The activation energies of degradation estimated from the Ozawa's method

Epoxy	E_d (kJ/mol)
MDES	190
MDAE0.5S	220
MDAE1.0S	231
MDAE1.5S	248
MDAE2.0S	268

$$\int_0^{\alpha} \frac{d\alpha}{(1-\alpha)^n} = \frac{1}{\Phi}\int_{T_0}^{T} Ae^{-E_d/RT}dT$$

$$F(\alpha) = \frac{AE_d}{\Phi R}P(\lambda) \tag{8}$$

where $F(\alpha)$, $P(\lambda)$ are the thermal degradation conversion and shift variable dependent function, respectively, E_d is the activation energy of thermal degradation, Φ is the heating rate (°C/min). Eq. (8) can be derived from the integral and taking its logarithmic form

$$\log F(\alpha) = \log\frac{AE_d}{R} - \log \Phi + \log P(\lambda)(E_d/RT)$$

Flynn and Wall, and Ozawa have proved that constant degree of conversion, i.e. independent of the heating rate at the rapid weight loss temperature (T_r), thus, Eq. (8) can be reduced to

$$E_d = -\frac{R}{C}\left[\frac{\Delta \log \Phi}{\Delta(1/T_r)}\right] \tag{9}$$

where C value is constant and with 0.475 or 0.457, either one will suit Eq. (9). The E_d value can be got from the straight line with a slope of the log Φ versus $1/T_r$ plot (in Fig. 11). Table 5 shows that the E_d of MDAES systems (with ODOPB advancement) is higher than MDES. It indicates the bulky pendant chain and ring compound rigid structure of ODOPB. Furthermore, the activation energy of thermal degradation increases with content of phosphorous, due to their higher degradation bond energy, resulting in the yield of a high thermal stability polymer.

4. Conclusion

The cheap material from the light oil-cracking product dicyclopentadiene (DCPD), which reacted with aluminum chloride to form carbocation, then reacts with 2,6-dimethylphenol to produce 2,6-dimethylphenol–DCPD novolac (MDN). In the preparation of 2,6-dimethylphenol–DCPD epoxy resin (MDE), an excess amount of epichlorohydrin (mole ratio: 10/1) was used in order to minimize high molecular weight species. Hence, the typical product contained ca. 98% by weight of the short-chain MDE. The curing kinetics of epoxy resins were studied by the Kissinger and Ozawa methods. The values of activation energy for curing behavior are quite close to kinetic model. Either the activation energy for curing or thermal degradation, the ODOPB-modified epoxy resins were higher than unmodified system. The phenylphosphonate structure interfered the molecular mobility and diffusion. In addition, the incorporation of bulky phenylphosphonate has resulted in the good flame retardancy and high thermal stability.

References

[1] Ho TH, Wang CS. J Appl Polym Sci 1994;54:13.
[2] Zanni-Deffarges MP, Shanahan MER. Int J Adhes Adhes 1995;15:137.
[3] Kagawa Y, Iba H, Tanaka M, Sato H, Chang T. Acta Mater 1998;46:265.
[4] Kotnarowska D. Prog Org Coat 1999;37:149.
[5] Wang CS, Lin CH. Polymer 2000;41:8579.
[6] Kuo DH, Chang CC, Su TY, Wang WK, Lin BY. J Eur Ceram Soc 2001;21:1171.
[7] Okamatsu T, Ochi M. Polymer 2002;43:721.
[8] Lin CH, Huang MJ, Wang CS. Polymer 2002;43:2959.
[9] Dang W, Kubouchi MY, Shuron S, Hideki TK. Polymer 2002;43:2953.
[10] Roizard X, Wery M, Kirmann J. Compos Struct 2002;56:223.
[11] Chin WK, Hsau MD, Tsai WC. J Polym Sci Part A Polym Chem 1995;33:373.
[12] Wang CS, Shieh JY. J Appl Polym Sci 1999;73:353.
[13] Shieh JY, Wang CS. J Polym Sci Part A Polym Chem 2002;40:369.
[14] Maiti S, Banerjee S, Palit SK. Prog Polym Sci 1993;18:227.
[15] Derouet D, Morvan F, Brosse C. J Appl Polym Sci 1996;62:1855.
[16] Sirrier H, Gorgier S, Borissov G. Eur Polym J 1990;26:73.
[17] Shau MD, Wang TS. J Polym Sci Part A Polym Chem 1996;34:384.
[18] Liu YL, Hsiu GH, Chiu YS. J Polym Sci Part A Polym Chem 1997;35:565.
[19] Cho CS, Fu SC, Chen LW, Wu TR. Polym Int 1998;47:203.
[20] Wang CS, Lin CH. J Polym Sci Part A Polym Chem 1999;37:3906.
[21] Wang CS, Lin CH. J Appl Polym Sci 2000;75:429.
[22] Liu YL, Hsiu GH, Chiu YS, Jeng RJ. J Appl Polym Sci 1996;61:613.
[23] Banks M, Ebdon JR, Johnson M. Polymer 1993;34:4547.
[24] Liu YL, Hsiu GH, Lee RH, Chiu YS. J Appl Polym Sci 1997;63:895.
[25] Jay R. Anal Chem 1964;36:667.
[26] Lin CH, Wang CS. Polymer 2001;42:1869.
[27] Ho TH, Leu TS. J Appl Polym Sci 2003;90:1066.
[28] Lin CH, Yang KZ, Leu TS, Lin CH, Sie JW. J Polym Sci Part A Polym Chem 2006;44:3847.
[29] Wang CS, Leu TS, Hsu KR. Polymer 1998;39(13):2921.
[30] Kissinger HE. Anal Chem 1957;29:1072.
[31] Ozawa TJ. Bull Chem Soc Jpn 1965;38:1881.
[32] Ozawa TJ. J Therm Anal 1970;2:301.
[33] Doyle CD. J Appl Polym Sci 1961;5:285.
[34] Flynn JH, Wall LA. Polym Lett 1966;4:323.